

KEK-TH-421
KEK preprint 94-159
HUPD-9417
December 1994

Charged Higgs mass bound from the $b \rightarrow s \gamma$ process in the minimal supergravity model

Toru GOTO¹ and Yasuhiro OKADA²

¹*Department of Physics, Hiroshima University
1-3-1 Kagamiyama, Higashi Hiroshima, 724 Japan*

²*Theory Group, KEK, Tsukuba, Ibaraki, 305 Japan*

Abstract

We study the constraint on the mass of the charged Higgs boson in the minimal supergravity model based on the recent measurement of the inclusive $b \rightarrow s \gamma$ decay. It is shown that the lower bound for the charged Higgs mass crucially depends on the sign of the higgsino mass parameter (μ). For $\mu < 0$, the bound exceeds 400 GeV when the ratio of two Higgs vacuum expectation values ($\tan \beta$) is larger than 10. No strong bound is obtained for $\mu > 0$ due to cancellations between charged Higgs and supersymmetric particle contributions. For $3 \lesssim \tan \beta \lesssim 5$, a charged Higgs lighter than 180 GeV is excluded by this process irrespective of the sign of μ .

Flavor changing neutral current (FCNC) processes play a unique role in searching for physics beyond the standard model (SM) of elementary particles. These processes are sensitive to virtual effects of new particles, since the FCNC processes in SM do not occur at the tree level. These processes can thus be more powerful than direct particle searches in putting constraints on the parameter space of various new physics. In particular, the radiative decay of the b quark, $b \rightarrow s \gamma$, deserves a special attention. It has been noticed that in a two Higgs doublet model (THDM) the charged Higgs boson can give a substantial contribution to the $b \rightarrow s \gamma$ rate [1, 2]. Recently, the CLEO group [3] has reported the first measurement of the inclusive $b \rightarrow s \gamma$ branching ratio $\text{Br}(b \rightarrow s \gamma) = (2.32 \pm 0.51 \pm 0.29 \pm 0.32) \times 10^{-4}$. In fact, this result constrains the mass of the charged Higgs boson in a certain type of THDM called Model II [1, 2] to be larger than 260 GeV [3].

The Higgs sector in the minimal supersymmetric (SUSY) extension of SM is a special case of Model II THDM. However, the above-mentioned limit cannot be directly applied, because SUSY particles can contribute to the $b \rightarrow s \gamma$ process in addition to the SM particles and the charged Higgs. It is a natural question to ask how the charged Higgs mass limit is modified in the SUSY extension of SM. Many authors have discussed the $b \rightarrow s \gamma$ process in SUSY [4]-[18]. Although the SM and the charged Higgs contribution to the $b \rightarrow s \gamma$ amplitude has the same sign, it is found that the SUSY loop can interfere either constructively or destructively with them. The limit for the charged Higgs mass from this process can be weakened by the effects of the SUSY particles.

The minimal supergravity model provides an attractive framework for SUSY extension of SM. In this model, masses and mixing parameters for SUSY particles can be expressed by a few soft SUSY breaking parameters as well as gauge and Yukawa coupling constants. The $b \rightarrow s \gamma$ branching ratio thus depends on much smaller number of free parameters compared to that in general SUSY standard models. It has been noticed [8, 13, 16] that the sign of the SUSY loop contributions with respect to those of the SM and charged Higgs is strongly correlated with the sign of the higgsino mass parameter *i.e.* the μ parameter in the minimal supergravity model.

In this paper, we compare the CLEO data with the prediction of the minimal supergravity model and determine the allowed region in the parameter space of the

model. Scanning the free parameter space extensively, we search for the constraint on the charged Higgs mass. It will be shown that the lower bound of the charged Higgs mass crucially depends on the sign of μ . The bound becomes much larger than that in the non-SUSY Model II THDM for $\mu < 0$, while no strong bound is obtained for $\mu > 0$.

The calculation of the $b \rightarrow s \gamma$ branching ratio has already been discussed extensively in the literature [2, 19, 20]. The decay rate for $b \rightarrow s \gamma$ normalized to the semileptonic decay rate is given by

$$\frac{\Gamma(b \rightarrow s \gamma)}{\Gamma(b \rightarrow c e \bar{\nu})} = \frac{1}{|V_{cb}|^2} \frac{6\alpha_{\text{QED}}}{\pi g(m_c/m_b)} |V_{ts}^* V_{tb} C_7^{\text{eff}}(Q)|^2, \quad (1)$$

$$C_7^{\text{eff}}(Q) = \eta^{16/23} C_7(M_W) + \frac{8}{3} (\eta^{14/23} - \eta^{16/23}) C_8(M_W) + C,$$

where $\eta = \alpha_s(M_W)/\alpha_s(Q)$, Q being the scale of the order of the bottom mass, and $g(z) = 1 - 8z^2 + 8z^6 - z^8 - 24z^4 \ln z$. C is a constant which depends on η . The above formula takes the leading order QCD corrections into account. The $C_7(M_W)$ and $C_8(M_W)$ are coefficients of the magnetic and chromomagnetic operators at M_W . The C term is induced by operator mixing in evolving from M_W to the low energy scale Q .

Ambiguities in the calculation are discussed in detail in Ref. [20]. The most important ambiguity comes from the choice of the renormalization scale Q . Varying Q between $m_b/2$ and $2m_b$ induces an ambiguity of $\pm 25\%$ for the branching ratio in SM. Other ambiguities include the choice of m_c/m_b (which affects the semileptonic rate) and the value of $\alpha_s(M_Z)$.

The coefficients $C_7(M_W)$ and $C_8(M_W)$ receive the following contributions at one loop: (i) the W and top quark loop, (ii) the charged Higgs and top quark loop, (iii) the chargino and up-type squark loops, (iv) the gluino and down-type squark loops and (v) the neutralino and down-type squark loops. The contribution from (v) is known to be very small [4], which we will ignore hereafter. The charged Higgs contribution depends on its mass and the ratio of the vacuum expectation values of the two Higgs doublets, *i.e.* $\tan \beta = \langle H_2^0 \rangle / \langle H_1^0 \rangle$, where H_1^0 and H_2^0 are the neutral component of the two Higgs doublets. The chargino and gluino loop contributions depend on the mass and mixing of the particles inside the loop. Although the squark mixing matrices are arbitrary parameters in a general SUSY standard model, they

can be calculated from the flavor mixing matrix of quarks (the Cabibbo-Kobayashi-Maskawa matrix) in the minimal supergravity model by solving the renormalization group equations for various soft SUSY breaking terms.

The soft SUSY breaking parameters at the GUT scale are the universal scalar mass (m_0), a parameter in the trilinear coupling of scalars (A_X), a parameter in the two Higgs coupling (B_X) and the gaugino mass (M_{gX}). We are assuming the GUT relation for the three gaugino masses *i.e.* the SU(3), SU(2) and U(1) gaugino mass parameters are equal at the GUT scale. Besides these soft SUSY breaking parameters, the superpotential contains the Yukawa coupling constants and the μ parameter. Given a value for the top mass and $\tan\beta$, we determine all the particle masses and mixings at the weak scale by solving relevant renormalization group equations with initial conditions at the GUT scale specified by the above parameters. We compute the Higgs effective potential at the weak scale and require that the electroweak symmetry is broken properly (the radiative breaking scenario). We include the one loop corrections to the effective potential induced by the Yukawa couplings for the third generation. The condition for radiative breaking with the correct scale reduces the number of free parameters to three for given $\tan\beta$ and m_t . We can think of these parameters as the charged Higgs mass (m_{H^\pm}), μ and M_2 (SU(2) gaugino mass) at the weak scale. For a given set of these five parameters, all other masses and mixings are thus calculable.

We now present the results of the $b \rightarrow s \gamma$ branching ratio. Besides the radiative breaking condition we require the following phenomenological constraints [21]:

1. The mass of any charged SUSY particle is larger than 45 GeV;
2. The sneutrino mass is larger than 41 GeV;
3. The gluino mass is larger than 100 GeV;
4. Neutralino search results at LEP [22], which require $\Gamma(Z \rightarrow \chi\chi) < 22$ MeV, $\Gamma(Z \rightarrow \chi\chi')$, $\Gamma(Z \rightarrow \chi'\chi') < 5 \times 10^{-5}$ GeV, where χ is the lightest neutralino and χ' is any neutralino other than the lightest one;
5. The lightest SUSY particle (LSP) is neutral;

6. The condition for not having a charge or color symmetry breaking vacuum [23].

In Fig. 1, we show the $b \rightarrow s \gamma$ branching ratio for $m_t = 175 \text{ GeV}^*$ and $\tan \beta = 5$. Each point in the figure corresponds to the value of the $b \rightarrow s \gamma$ branching ratio for each scanned point in the parameter space compatible with the above conditions. This branching ratio includes the chargino and gluino loop contributions as well as the SM and the charged Higgs loop. The line in the figure represents the branching ratio when only the SM and charged Higgs contributions are retained. We notice that the points are divided by this line. In fact, the points above and below this line correspond to $\mu < 0$ and $\mu > 0$ cases respectively[†]. This confirms the assertion [8, 13, 16] that the sign of μ determines whether the SUSY contribution enhances or suppresses the $b \rightarrow s \gamma$ branching ratio.

We show the excluded region in the $\tan \beta$ and m_{H^\pm} space in Fig. 2a and Fig. 2b. The two branches $\mu > 0$ and $\mu < 0$ are separately plotted. The excluded region is determined using the CLEO result $1 \times 10^{-4} < \text{Br}(b \rightarrow s \gamma) < 4 \times 10^{-4}$. In order to take account of the theoretical uncertainties we have calculated the $b \rightarrow s \gamma$ branching ratio by varying the renormalization scale Q between $m_b/2$ and $2m_b$. To be conservative, we also allow an additional 10% uncertainty. In the calculation we have used $\alpha_s(m_Z) = 0.116$, $m_c/m_b = 0.3$ and $m_b = 4.25 \text{ GeV}$. We regard a point in $(\tan \beta, m_{H^\pm})$ space excluded when the branching ratio cannot be within the CLEO bound for any choice of other parameters (*i.e.* μ and M_2) even if we consider the above-mentioned theoretical ambiguities. We also show in these figures the lower bound of the charged Higgs mass when only the SM and the charged Higgs contributions are retained. In comparison, the excluded region in minimal supergravity becomes larger when $\mu < 0$. The bound reaches 400 GeV for $\tan \beta > 10$. For $\mu > 0$, the $b \rightarrow s \gamma$ process is not very effective in constraining the charged Higgs mass, because the charged Higgs contribution can be completely cancelled by SUSY particle contributions.

We combine the two branches in Fig. 3. The region where $3 \lesssim \tan \beta \lesssim 5$ and the charged Higgs is lighter than 180 GeV is excluded irrespective of the sign of

*This top quark mass is the $\overline{\text{MS}}$ running mass at $Q = M_Z$. This mass coincides with the pole mass within a few percent [24].

[†] Our convention of the sign of μ is opposite to those in Refs. [13] and [16].

μ^\ddagger . Before including the $b \rightarrow s \gamma$ constraint, this region was allowed only for $\mu < 0$ because of the phenomenological and radiative breaking conditions. The $b \rightarrow s \gamma$ process now completely excludes this region.

The reason for the strong dependence on μ can be understood as follows. For the chargino and up-type squark loop the most important contribution comes from the loop diagram with the top and bottom Yukawa coupling constants. This diagram is proportional to a product of the left-right mixing parameter of the stops, *i.e.* $A_t - \mu \cot \beta$, and the higgsino mixing parameter μ . The parameter A_t is determined by A_X and M_{gX} through the renormalization group equations. An interesting observation is that for such a high value of the top quark mass as considered here A_t is almost independent of A_X and proportional to M_{gX} . Moreover, the $\mu \cot \beta$ term is suppressed for $\tan \beta > 3$. Therefore, the amplitude from this sector is proportional to a product of the gaugino mass and the higgsino mass parameter in a very good approximation. A similar consideration applies to the gluino and down-type squark loop. In this case a sizable contribution can arise when the graph involves the left-right mixing in the sbottom sector, especially for a large value of $\tan \beta$. Then, the amplitude is proportional to a product of the gluino mass (M_3) and the sbottom mixing parameter, *i.e.* $A_b - \mu \tan \beta$. For a large value of $\tan \beta$ the latter parameter is governed by the $\mu \tan \beta$ term. Here again, the contribution to the amplitude is almost proportional to the product of the gaugino mass and the higgsino mass parameter. In both cases, the SUSY contribution enhances (suppresses) the SM amplitude when $\mu < 0$ ($\mu > 0$).

Let us discuss generalizations of our results. First, we consider the situation when LEP II fails to find any SUSY particle. Then the lower bounds for the charged SUSY particle masses rise to about 90 GeV. The excluded region of the charged Higgs mass and $\tan \beta$ are shown in Fig. 4a and Fig. 4b. We can see that the allowed region by the phenomenological constraint and radiative breaking condition is shifted to higher values of the charged Higgs mass. For $\mu < 0$, the line for the lower bound from the $b \rightarrow s \gamma$ constraint is unchanged and still a large portion of the parameter space is excluded. Therefore the present $b \rightarrow s \gamma$ constraint can be stronger than the constraint provided by the LEP II search in determining an allowed parameter region in the minimal supergravity model.

[‡] A similar observation was made in Ref. [13] for a special choice of the B parameter.

Next, we would like to study how strongly the results depend on the assumption of the universal scalar mass at the GUT scale. By defining the tree Higgs potential as;

$$V_{\text{tree}} = (\Delta_1^2 + \mu^2)|H_1|^2 + (\Delta_2^2 + \mu^2)|H_2|^2 - B\mu(H_1H_2 + H_1^*H_2^*) + (D \text{ terms}), \quad (2)$$

we have changed the initial condition for the Higgs soft breaking term, Δ_1^2 , Δ_2^2 as $\Delta_2^2 = r \cdot m_0^2$, $\Delta_1^2 = m_0^2$, where m_0^2 is an universal scalar mass for squarks and sleptons. We have introduced a parameter r to relax the assumption that all the scalar fields have a common soft SUSY breaking mass. In this way we can change the parameter space allowed by the requirement of the radiative electroweak symmetry breaking. Although the allowed parameter region in μ - M_2 space is changed for various choice of r (we varied r between 0.1 and 10), the situation that the charged Higgs mass is strongly constrained only for $\mu < 0$ remains true for any choice of r . As an example, the bound on the charged Higgs mass from the $b \rightarrow s \gamma$ process is shown in Fig. 5a and Fig. 5b for the choice $r = 4$. These analyses suggest that our results are independent of the details of the radiative breaking mechanism.

Finally, we will consider how the results depends on the top mass. It turns out that the correlation between the sign of μ and the sign of the $b \rightarrow s \gamma$ amplitude remains unchanged, although the numerical value of the charged Higgs mass bound depends on m_t . In the case of $m_t = 150$ GeV, where the lower bound of the charged Higgs mass without SUSY contributions is about 200 GeV, the charged Higgs mass bound becomes 220 GeV for $7 \lesssim \tan\beta \lesssim 25$ and reaches about 380 GeV for $\tan\beta = 35$ for $\mu < 0$. For $\mu > 0$ the $b \rightarrow s \gamma$ process is not effective to put constraints on the charged Higgs mass, just as in the case of $m_t = 175$ GeV.

To summarize, we have shown that for $\mu < 0$ the lower bound of the charged Higgs mass increases compared to that in the Model II THDM. On the other hand, for $\mu > 0$, the $b \rightarrow s \gamma$ process cannot put useful constraints on the allowed range of the charged Higgs mass because it is possible that the charged Higgs contribution is completely cancelled by other SUSY contributions. We have also pointed out that a parameter region corresponding to the charged Higgs mass less than 180 GeV and $3 \lesssim \tan\beta \lesssim 5$ is excluded by the $b \rightarrow s \gamma$ process irrespective of the sign of μ .

The authors would like to thank K. Hikasa and T. Yanagida for reading the manuscript carefully and giving useful comments. The work of Y. O. is supported

in part by the Grant-in-aid for Scientific Research from the Ministry of Education,
Science and Culture of Japan.

References

- [1] T.G. Rizzo, *Phys. Rev. D* **38** (1988) 820;
W.-S. Hou and R.S. Wiley, *Phys. Lett. B* **202** (1988) 591;
C.Q. Geng and J.N. Ng, *Phys. Rev. D* **38** (1988) 2857;
V. Barger, J.L. Hewett and R.J.N. Phillips, *Phys. Rev. D* **41** (1990) 3421.
- [2] B. Grinstein, R. Springer, and M. Wise, *Nucl. Phys. B* **339** (1990) 269.
- [3] B. Barish *et al.*, (CLEO Collaboration), Contribution to the International Conference on High Energy Physics, Glasgow, July 20–27, 1994, preprint CLEO CONF 94-1.
- [4] S. Bertolini, F. Borzumati, A. Masiero, and G. Ridolfi, *Nucl. Phys. B* **353** (1991) 591.
- [5] N. Oshimo, *Nucl. Phys. B* **404** (1993) 20.
- [6] J. Hewett, *Phys. Rev. Lett.* **70** (1993) 1045;
V. Barger, M. Berger, and R.J.N. Phillips, *Phys. Rev. Lett.* **70** (1993) 1368.
- [7] R. Barbieri and G.F. Giudice, *Phys. Lett. B* **309** (1993) 86.
- [8] J.L. Lopez, D.V. Nanopoulos, and G.T. Park, *Phys. Rev. D* **48** (1993) 974;
J.L. Lopez, D.V. Nanopoulos, G.T. Park, and A. Zichichi, *Phys. Rev. D* **49** (1994) 355.
- [9] Y. Okada, *Phys. Lett. B* **315** (1993) 119.
- [10] R. Garisto and J.N. Ng, *Phys. Lett. B* **315** (1993) 372.
- [11] M.A. Diaz, *Phys. Lett. B* **322** (1994) 207.
- [12] F.M. Borzumati, *Z. Phys. C* **63** (1994) 291.
- [13] S. Bertolini and F. Vissani, *SISSA preprint* SISSA 40/94/EP, March 1994.
- [14] J. Wu, P. Nath, and R. Arnowitt, *Texas A-M preprint* CTP-TAMU-03-94, March 1994;

- P. Nath and A. Arnowitt, *Phys. Lett.* **B 336** (1994) 395; *CERN preprint* CERN-TH-7363-94, July 1994.
- [15] F.M. Borzumati, M. Drees, and M.M. Nojiri, *KEK preprint* KEK-TH-400, June 1994.
- [16] J.L. Lopez, D.V. Nanopoulos, X. Wang, and A. Zichichi, *CERN preprint* CERN-TH-7335-94, June 1994.
- [17] G. Kane, C. Kolda, L. Roszkowski, and D. Wells, *Phys. Rev.* **D 49** (1994) 6173.
- [18] M. Carena, M. Olechowski, S. Pokorski, and C.E.M. Wagner, *Nucl. Phys.* **B 426** (1994) 269.
- [19] M. Misiak, *Phys. Lett.* **B 296** (1991) 161; *Nucl. Phys.* **B 393** (1993) 23.
- [20] A.J. Buras, M. Misiak, M. Münz and S. Pokorski, *Nucl. Phys.* **B 424** (1994) 374.
- [21] L. Montanet, *et al.*, (Particle Data Group), *Phys. Rev.* **D 50** (1994) 1173.
- [22] D. Decamp, *et al.*, (ALEPH Collaboration), *Phys. Rep.* **216** (1992) 253.
- [23] J.P. Derendinger and C.A. Savoy, *Nucl. Phys.* **B 237** (1984) 307.
- [24] A.J. Buras, M. Jamin and P.H. Weisz, *Nucl. Phys.* **B 347** (1990) 491.

Figure Captions

FIG. 1 $b \rightarrow s \gamma$ branching ratio for $m_t = 175$ GeV and $\tan\beta = 5$. Each dot corresponds to a sample point which satisfies radiative breaking and phenomenological constraints (see text). Solid line represents the branching ratio calculated with the SM and charged Higgs contributions only (Model II THDM). Dot-dashed line represents the SM value.

FIG. 2a Excluded region in the $\tan\beta$ and m_{H^\pm} space for $\mu < 0$. Each line represents the lower bound for the charged Higgs mass; solid line: all constraints included; dashed line: without $b \rightarrow s \gamma$ constraint; dot-dashed line: Model II THDM with $b \rightarrow s \gamma$ constraint.

FIG. 2b Same as Fig. 2a for $\mu > 0$.

FIG. 3 Excluded region in the $\tan\beta$ and m_{H^\pm} space irrespective of the sign of μ . The meanings of the lines are the same as those in Fig. 2a.

FIG. 4a Excluded region in the $\tan\beta$ and m_{H^\pm} space for $\mu < 0$ with LEP II constraint. The meanings of the lines are the same as those in Fig. 2a.

FIG. 4b Same as Fig. 4a for $\mu > 0$.

FIG. 5a Excluded region in the $\tan\beta$ and m_{H^\pm} space for $\mu < 0$ when the initial condition for Δ_2^2 is taken to be $4 \cdot m_0^2$. The meanings of the lines are the same as those in Fig. 2a.

FIG. 5b Same as Fig. 5a for $\mu > 0$.

Figures

FIG. 1: $b \rightarrow s \gamma$ branching ratio for $m_t = 175$ GeV and $\tan\beta = 5$. Each dot corresponds to a sample point which satisfies radiative breaking and phenomenological constraints (see text). Solid line represents the branching ratio calculated with the SM and charged Higgs contributions only (Model II THDM). Dot-dashed line represents the SM value.

FIG. 2a: Excluded region in the $\tan\beta$ and m_{H^\pm} space for $\mu < 0$. Each line represents the lower bound for the charged Higgs mass; solid line: all constraints included; dashed line: without $b \rightarrow s \gamma$ constraint; dot-dashed line: Model II THDM with $b \rightarrow s \gamma$ constraint.

FIG. 2b: Same as Fig. 2a for $\mu > 0$.

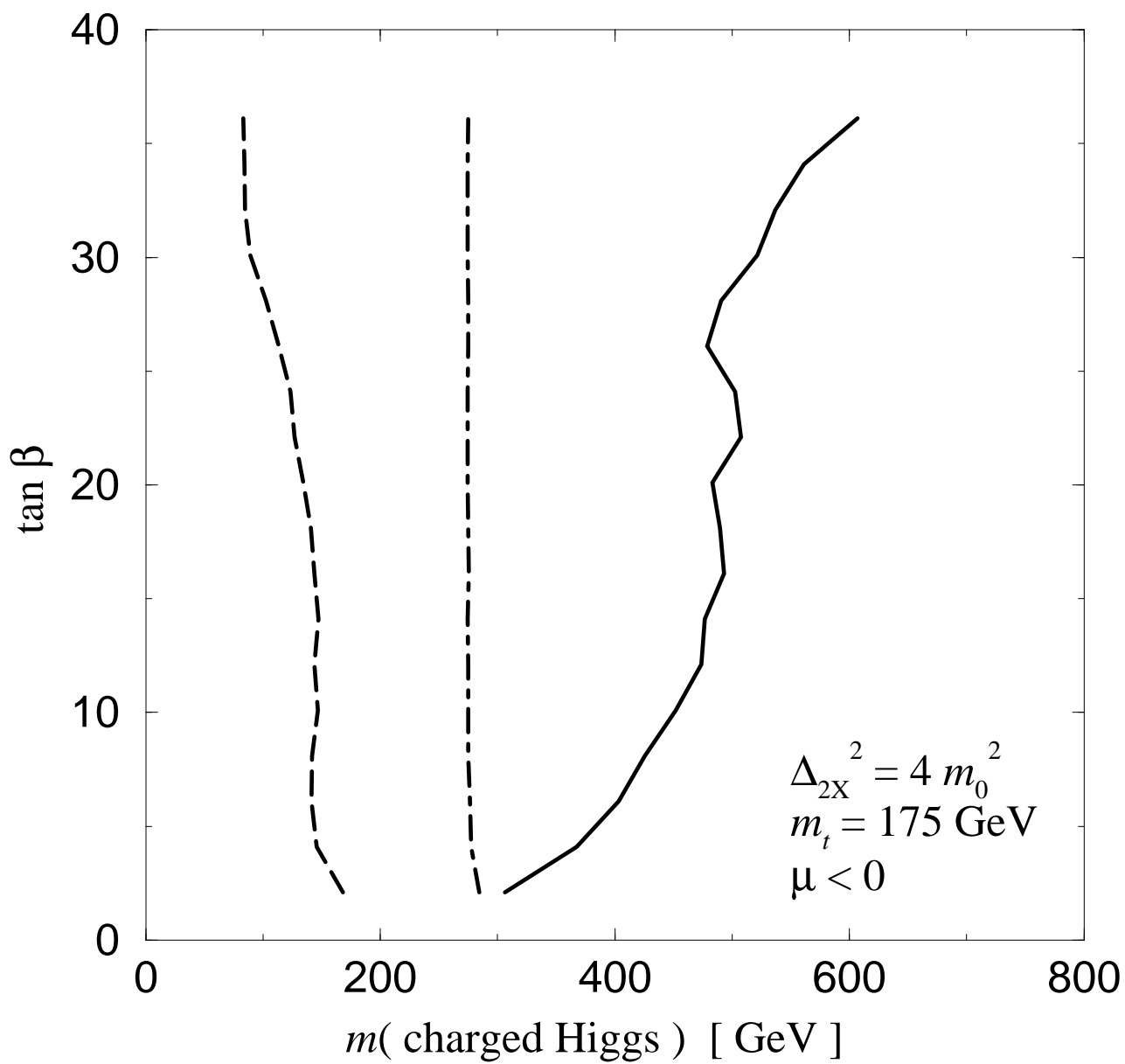
FIG. 3: Excluded region in the $\tan\beta$ and m_{H^\pm} space irrespective of the sign of μ . The meanings of the lines are the same as those in Fig. 2a.

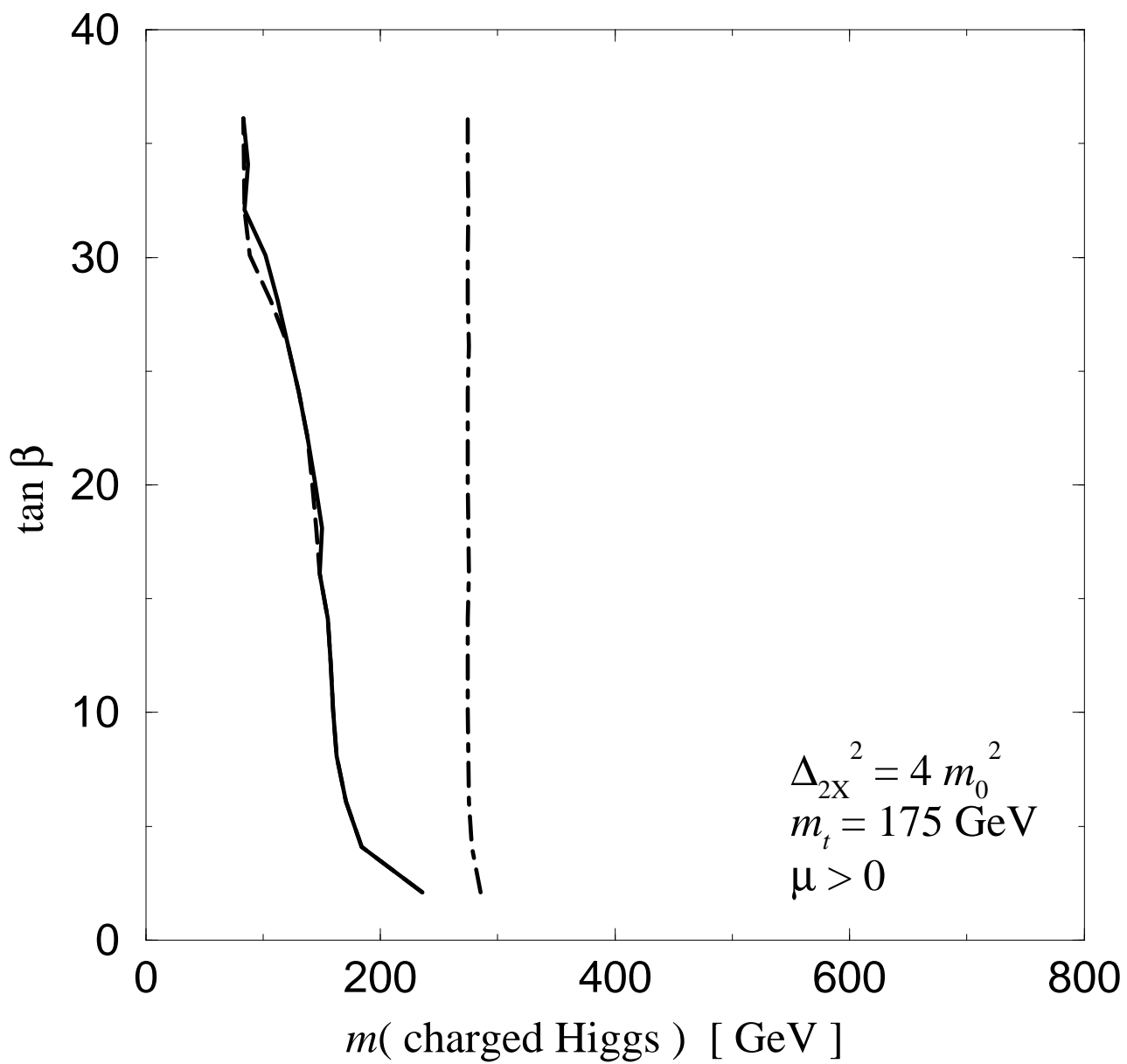
FIG. 4a: Excluded region in the $\tan\beta$ and m_{H^\pm} space for $\mu < 0$ with LEP II constraint. The meanings of the lines are the same as those in Fig. 2a.

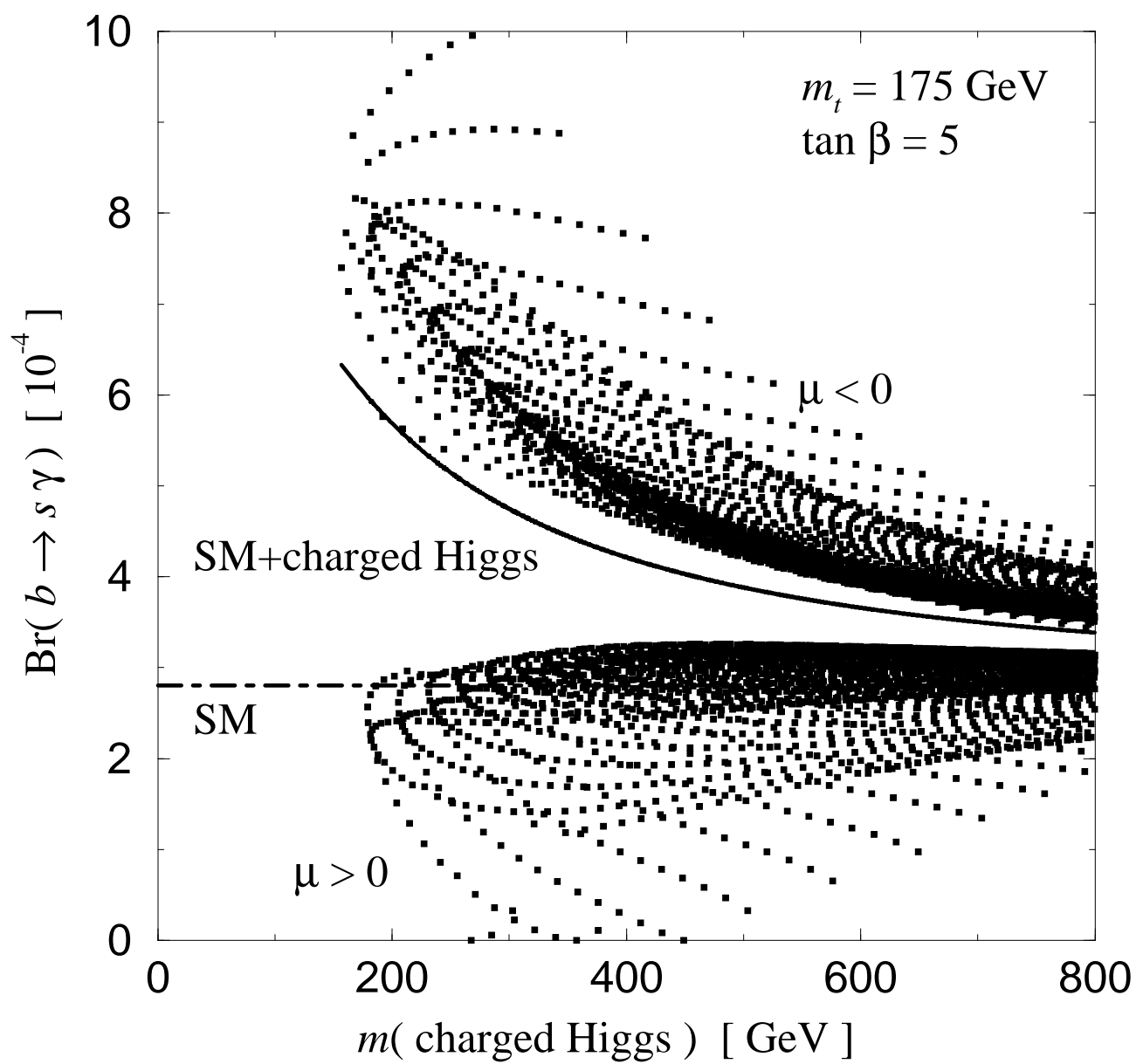
FIG. 4b: Same as Fig. 4a for $\mu > 0$.

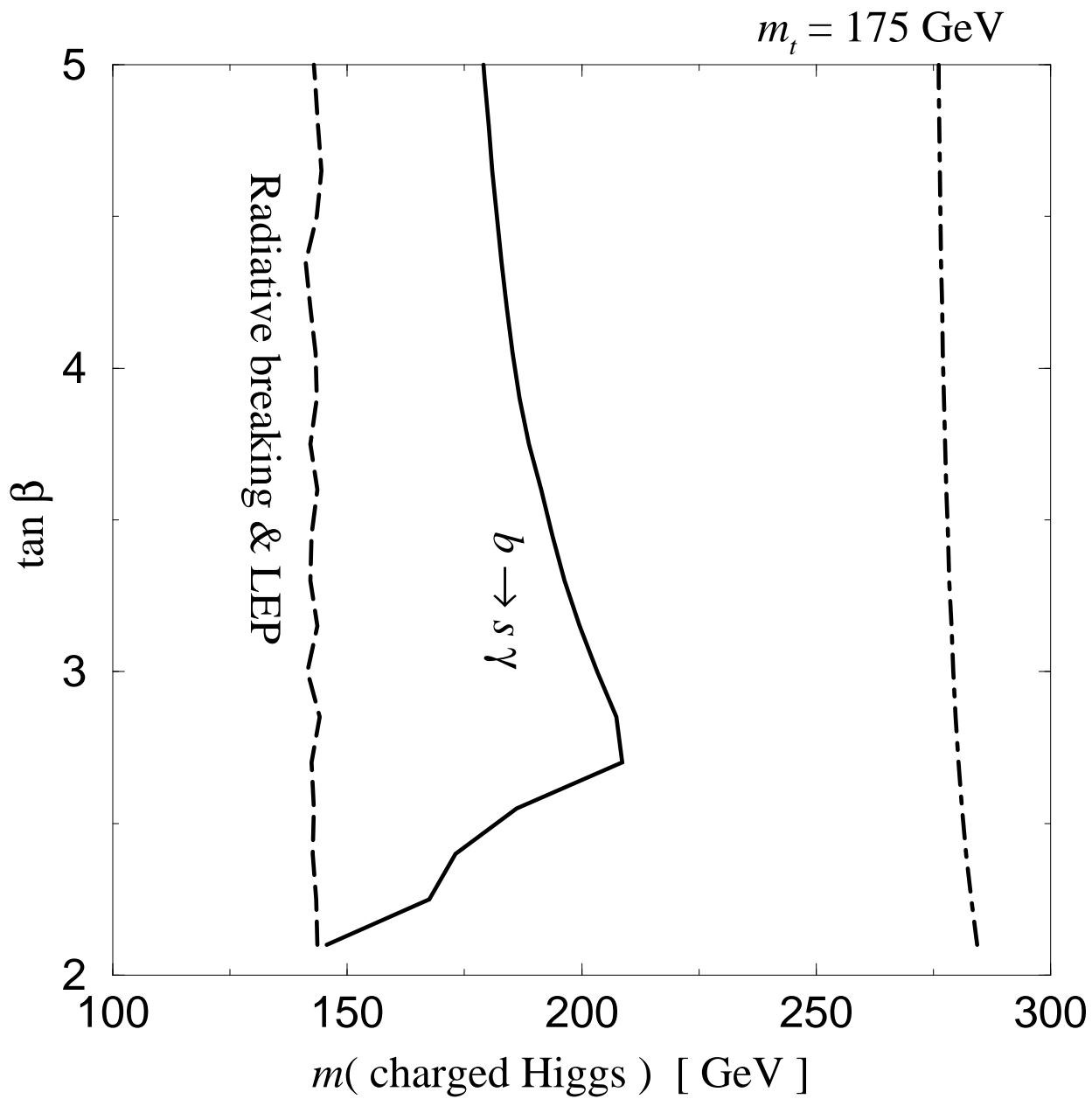
FIG. 5a: Excluded region in the $\tan\beta$ and m_{H^\pm} space for $\mu < 0$ when the initial condition for Δ_2^2 is taken to be $4 \cdot m_0^2$. The meanings of the lines are the same as those in Fig. 2a.

FIG. 5b: Same as Fig. 5a for $\mu > 0$.









This figure "fig1-1.png" is available in "png" format from:

<http://arxiv.org/ps/hep-ph/9412225v1>

This figure "fig2-1.png" is available in "png" format from:

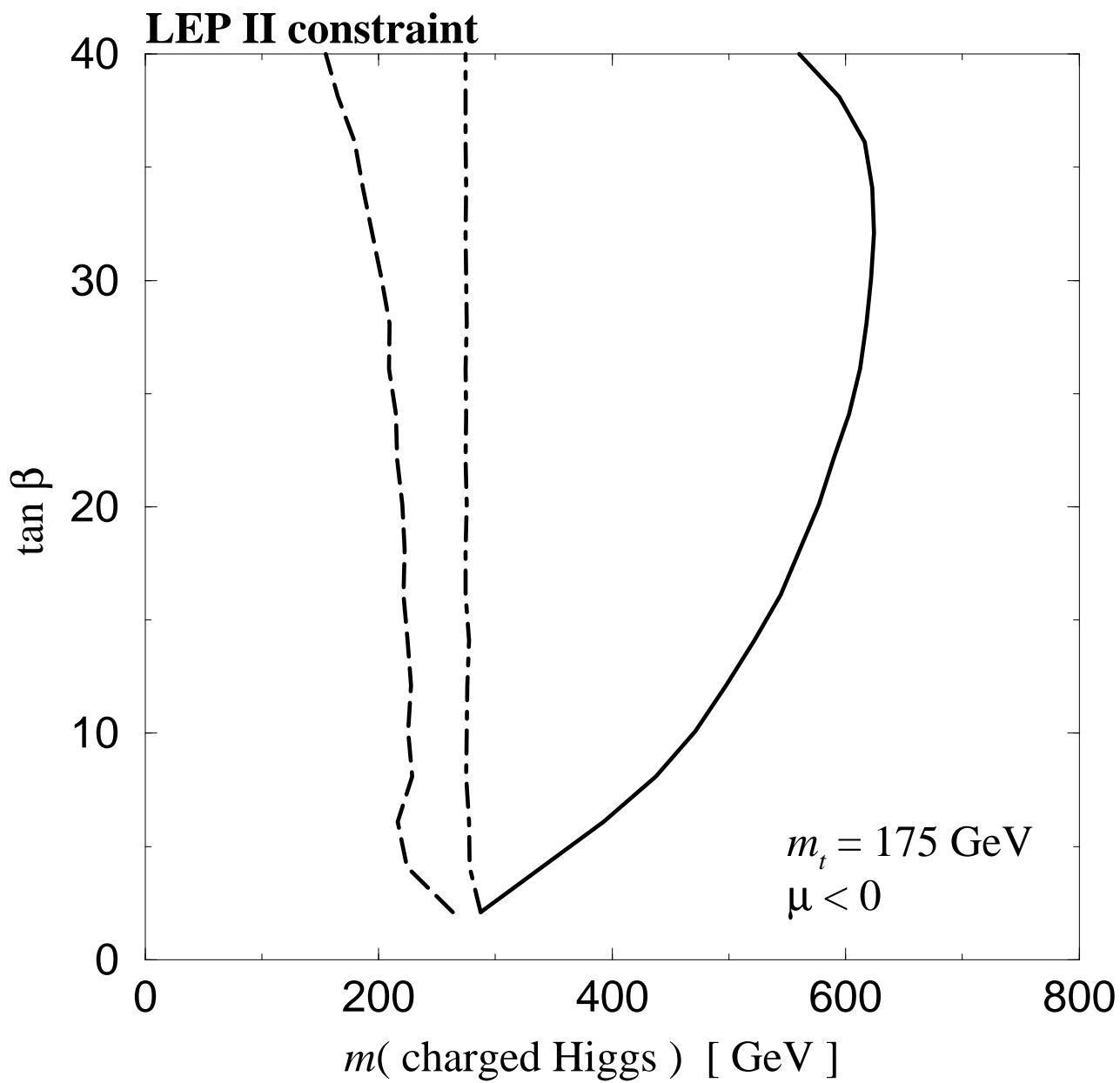
<http://arxiv.org/ps/hep-ph/9412225v1>

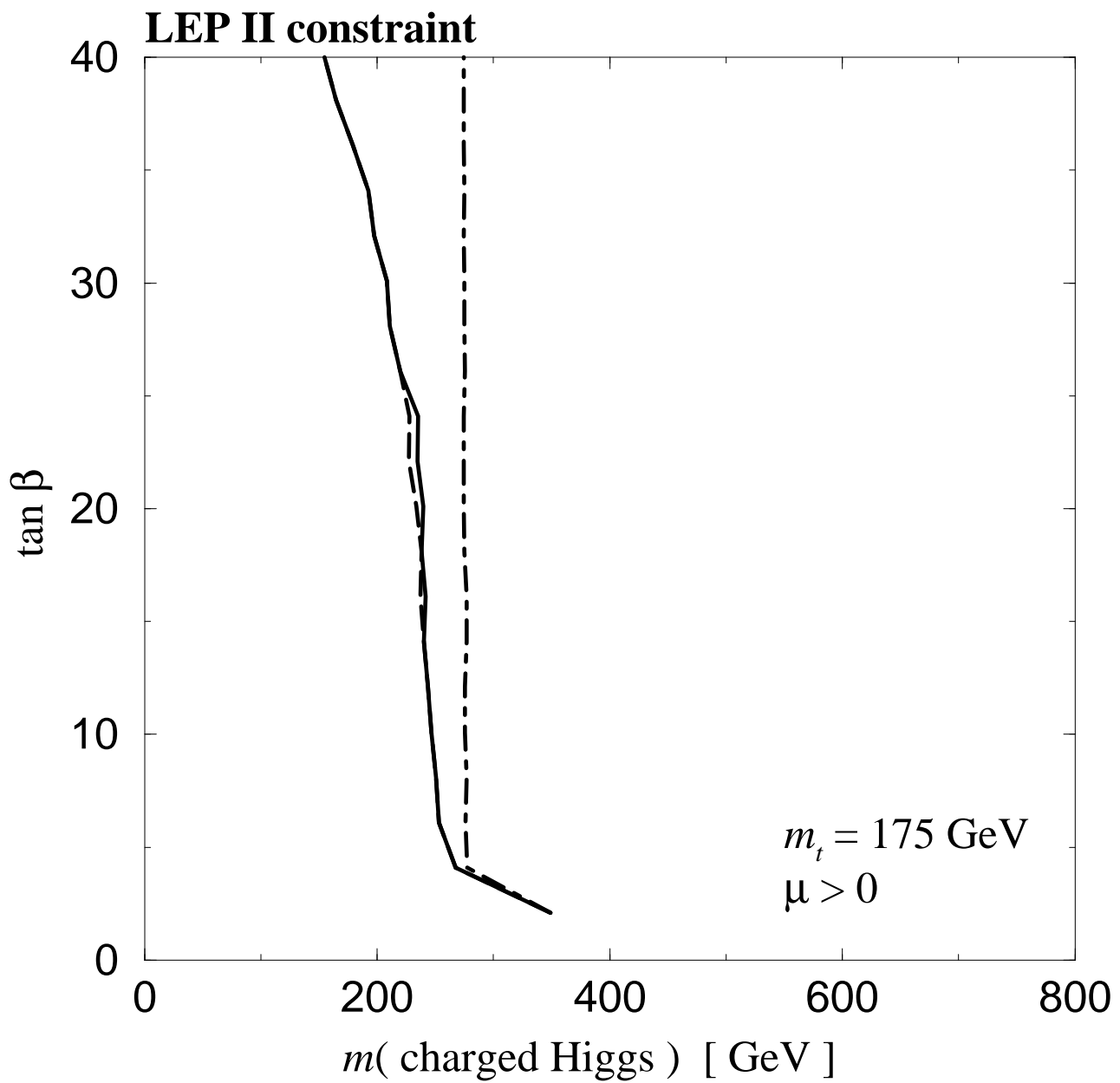
This figure "fig1-2.png" is available in "png" format from:

<http://arxiv.org/ps/hep-ph/9412225v1>

This figure "fig2-2.png" is available in "png" format from:

<http://arxiv.org/ps/hep-ph/9412225v1>





This figure "fig1-3.png" is available in "png" format from:

<http://arxiv.org/ps/hep-ph/9412225v1>

This figure "fig2-3.png" is available in "png" format from:

<http://arxiv.org/ps/hep-ph/9412225v1>

This figure "fig1-4.png" is available in "png" format from:

<http://arxiv.org/ps/hep-ph/9412225v1>

This figure "fig1-5.png" is available in "png" format from:

<http://arxiv.org/ps/hep-ph/9412225v1>

